ARTICLE

Preparation and Optical Properties of (Nanometer MCM-41)-CdS Composite Materials

Qing-zhou Zhai*, Yue-xiang Liu

Research Centre for Nanotechnology, Changchun University of Science and Technology, Changchun 130022, China

(Dated: Received on May 20, 2006; Accepted on August 13, 2006)

The nanometer and micrometer molecular sieves MCM-41 were prepared by a hydrothermal method. Cadmium (II) was exchanged into the molecular sieves by ion-exchange, and thioacetamide was then used as a precursor of hydrogen sulfide for sulphidizing the (MCM-41)-cadmium samples to prepare the host-guest composite materials (MCM-41)-CdS. By means of chemical analysis, powder X-ray diffraction, infrared spectroscopy, low temperature nitrogen adsorption-desorption technique, solid state diffuse reflectance absorption spectroscopy and luminescence, the prepared materials were characterized. The chemical analysis shows that the guest is successfully trapped in the molecular sieves. The powder X-ray diffraction suggests that the frameworks of the molecular sieves in the prepared host-guest composite materials are retained during the preparative process. They are intact and the degrees of crystallinity are still very high. The infrared spectra show that the frameworks of the prepared host-guest materials keep intact. The low temperature nitrogen adsorption-desorption studies indicate that the pore volumes, the pore sizes and the surface areas of the prepared composite materials decrease relative to those of the MCM-41 molecular sieve hosts. This shows that the guests are successfully encapsulated in the channels of the molecular sieves. The solid state diffuse reflectance absorption spectra of the prepared host-guest composites show some blue-shifts relative to that of bulk cadmium sulfide, indicating that the guests are trapped in the channels of the molecular sieves. This shows the obvious stereoscopic confinement effect of the molecular sieve host on the nanometer cadmium sulfide guest. The (nanometer MCM-41)-CdS and (micrometer MCM-41)-CdS samples show obvious luminescence.

Key words: Host-guest nanocomposite material, Nanometer MCM-41 molecular sieve host, Cadmium sulfide guest, Optical property

I. INTRODUCTION

MCM-41 molecular sieves are a new family of mesoporous molecular sieves and exhibit a periodic pore system [1,2]. They can be catalysts, adsorbents, etc., and have potential practical performance. Therefore, studies on MCM-41 are of great interest [3]. The MCM-41 molecular sieves have large channels, which can be ideal hosts for the incorporation of guest. According to their big and adjusted pore diameters, high specific surface, large adsorptive capacity and good thermal stability, MCM-41 molecular sieves have already shown their great potentiality and diversity in adsorption, separation and catalytic activity [3,4]. The modification of MCM-41 by Al [5-7], Ti [8,9], Cu [10], Ni [11], B [12], Fe [13], Mn [14], NiO, MoO_3 [15], surface silylation [16], metallocene complex [17], or organic functionalized group [18,19] is very active. In recent years, the studies on nanomaterials have been a very popular topic [20-29]. A nanometer MCM-41 molecular sieve [30] was synthesized in 2001. Some sulfides have potential as optical materials and then can be used as the guests to be incorporated into their molecular sieve hosts [31]. Cadmium sulfide is a type of semiconductor material, and it is used as an important candidate material for the conversion of solar energy and photocatalysis. The preparative methods of this kind of molecular sieve host-sulfide guest composite material were mostly the sulfidation of cadmium (II) exchanged molecular sieves by using hydrogen sulfide with toxicity as a sulfur source [31,32]. Here, we use a novel *in situ* method of sulfidation by a hydrothermal method, and thiacetamide is adopted as a precursor of hydrogen sulfide in the hydrothermal reaction to sulfurize the samples. The corresponding reaction is $CH_3CSNH_2+H_2O=CH_3COONH_4+H_2S$ [33], $Cd^{2+}+H_2S=CdS+2H^+$. In this way the direct use of hydrogen sulfide can be avoided and hydrothermal method is used to produce hydrogen sulfide and the operation is easy. The channels of the MCM-41 are in the nanosize range, which can precisely control the size of the nanoparticles incorporated [34,35]. The formation method of CdS nanoparticles in the channels of the MCM-41 molecular sieve is described in this paper. The (micrometer MCM-41)-CdS and (nanometer MCM-41)-CdS samples were prepared for comparison. Chemical analysis, powder X-ray diffraction, infrared spectroscopy, low temperature nitrogen adsorption-desorption technique, solid state diffuse reflectance absorption spectroscopy, and luminescence were used to characterize the prepared materials.

*Author to whom correspondence should be addressed. E-mail: Zhaiqingzhou@sohu.com, Zhaiqingzhou@hotmail.com

II. EXPERIMENTS

A. Reagents

The following reagents were used: tetraethyl orthosilicate (TEOS, Fluka); cetyltrimethylammonium bromide (CTMAB, Changzhou Xinhua Research Institute for Reagent); cadmium acetate (Shanghai Chemical Co., Ltd., Chinese Medicine Group); thiacetamide (Shanghai Lingfeng Chemical Co., Ltd); sodium hydroxide (Kaiyuan Kangyuan Chemical Plant); ammonia solution (Beijing Chemical Plant); ethanol (Liaobei Chemical Plant); cadmium sulfide (Beijing Chemical Plant). All reagents used were analytical grade. Doubly deionized water was used in the experiments.

B. Preparation of nanometer and micrometer MCM-41 molecular sieves

The nanometer MCM-41 and micrometer MCM-41 molecular sieve hosts were synthesized by a hydrothermal method using tetrathylorthosilicate as the silica source and cetyltrimethylammonium bromide as the structure-directing agent. A 1.0 g of CTMAB was added to 480 mL of deionized water at 80 °C under vigorous stirring. When the solution became homogeneous, 3.5 mL of 2 mol/L sodium hydroxide (for nanometer MCM-41) solution or 79 mL of 25% (V/V) ammonia solution (for micrometer MCM-41) solution was added with stirring. After the solution became homogeneous, 5 mL of TEOS was slowly added, giving rise to a white slurry. Then the reaction mixture was kept at 80 °C for 2 h. The resulting solid was recovered by filtration, extensively washed with deionized water, and dried at ambient temperature. The template was removed by calcination at 500 °C for 4 h. The prepared powder was MCM-41 molecular sieve, which was designated as S_1 (for nanometer MCM-41) or S_2 (for micrometer MCM-41) [30].

C. Preparation of nanocomposite materials

Nanometer or micrometer molecular sieves were added into different ethanol solutions of the cadmium acetate containing 2 mol /L of cadmium(II) with stirring for 4 h at ambient temperature. Then the above substances were filtered and washed. After that, the obtained solids were dried at 60 °C for 4 h. 0.4076 g thiacetamide and an appropriate amount of the above dried solid particles were mixed in 30 mL of deionized water. The mixed solution was sealed in an autoclave and heated at 80 °C for 48 h, then the resulting product was distilled and washed. The obtained solid sample was dried at 60 °C for 12 h. The resulting solid host-guest composite materials were designed as (nanometer MCM-41)-CdS (S_1-CdS) or (micrometer MCM-41)-CdS (S_2-CdS), respectively.

III. CHARACTERIZATION

The analysis of cadmium was carried out on a Hitachi Z-8000 polarized Zeeman atomic absorption spectrophotometer. The content of sulfur was measured by gravimetric analysis. Determination of silicon in molecular sieves was made by molybdosilicate blue photometry [36]. The powder X-ray diffraction patterns of the samples were recorded with a Siemens D5005 X-ray powder diffractometer, where a Cu Kα (λ=0.15418 nm and operating at 30 kV and 20 mA) was used as an X-ray source. The sample was scanned from 0.4° to 10° (2θ) with a count of 1 s at each point. The step width employed was 0.02° in 2θ. The infrared spectra were recorded on a Nicolet 5DX-FTIR spectrometer using KBr pellet technique. A typical pellet contains about 1wt% sample diluted by potassium bromide. Nitrogen adsorption and desorption isotherms were obtained at 77 K on a Micromeritics ASAP 2010M instrument. The surface area was estimated by the Brunauer-Emmett-Teller (BET) method [37], and the pore distribution was determined using the Barett-Joyner-Halenda (BJH) method [38]. The TEM images were recorded with a JEOL 2010 transmission electron microscope. For TEM analysis, specimens were prepared by dispersing the as-obtained powder in alcohol and then placing a drop of the suspension on a copper grid coated with a transparent graphite, followed by drying. The UV-Vis absorption spectra were measured using a Perkin-Elmer Lambda spectrophotometer. The luminescence measurements were performed on a SPEX-FL-2T2 double grating fluorometer at room temperature.

IV. RESULTS AND DISCUSSION

A. Chemical analysis

The results of chemical analysis show that the molecular formulas in terms of the contents of of S_1-CdS and S_2-CdS are $Cd_2S_{13}Si_{248}O_{873}$ and $Cd_2S_9Si_{345}O_{1050}$, respectively. This indicates that the guest was encapsulated in the host-guest composite materials prepared.

B. XRD analysis

The X-ray diffraction patterns of the materials are shown in Fig.1 and Fig.2. All the materials consist of the hexagonal ordered structure. The Bragg peaks can be attributed to (100), (110), (200) and (210) of the typical MCM-41 material, respectively [30], suggesting perfect long-range order in these materials. The lattice parameter a_0 was calculated in terms of the equation $a_0=2/\sqrt{3}d_{100}$. The d-spacing and a_0 are shown in Table I.

Figure 1 (a) and (c) show the X-ray diffraction patterns of the uncalcined micrometer and nanometer molecular sieve MCM-41, respectively. Figure 1 (b) and

ISSN 1003-7713/DOI:10.1360/cjcp2007.20(1).83.7

TABLE I The pore structure parameters of the samples

Sample	d_{100}/nm	a_0[a]/nm	BET surface area/(m^2/g)	Pore volume[b]/(cm^3/g)	Pore size[c]/nm
S_1	3.34	3.85	960.90	0.566	2.29
S_1-CdS	3.63	4.17	642.55	0.453	2.13
S_2	3.59	4.13	1047.89	0.778	2.65
S_2-CdS	4.19	4.84	785.99	0.584	2.52

[a] $a_0=2/\sqrt{3}d_{100}$.
[b] BJH adsorption cumulative volume of pores.
[c] Pore size calculated from the adsorption branch.

(d) are XRD patterns for the corresponding molecular sieves calcined. It can be seen that the intensities of the diffraction peaks of the calcined nanometer and micrometer MCM-41 molecular sieve samples (Fig.1 (b) and (d)) increased compared with the corresponding uncalcined samples (Fig.1 (a) and (c)). The corresponding d-spacing of the calcined micrometer and nanometer MCM-41 sample (Fig.1 (b) and (d)) is higher than that of corresponding uncalcined samples (Fig.1 (a) and (c)). This shows that after calcination the long-range order in the calcined samples is better than that in the uncalcined samples. In comparison with the diffraction intensity of the micrometer MCM-41, the nanometer MCM-41 intensity is weaker. The degree of crystallinity of the nanometer MCM-41 is smaller than that of the micrometer MCM-41. A comparison of the X-ray diffraction patterns for the host-guest composite materials and host materials is shown in Fig.2. Compared with the corresponding host, the diffraction angles of the (micro MCM-41)-CdS and (nano MCM-41)-CdS samples shift slightly to lower angles. The characteristic diffraction peaks of the MCM-41 of the corresponding host-guest composite materials are retained. This shows that the incorporation of the guest does not destroy the structures of the host mesoporous materials. The hexagonal ordered structure of the MCM-41 is retained in the pro-

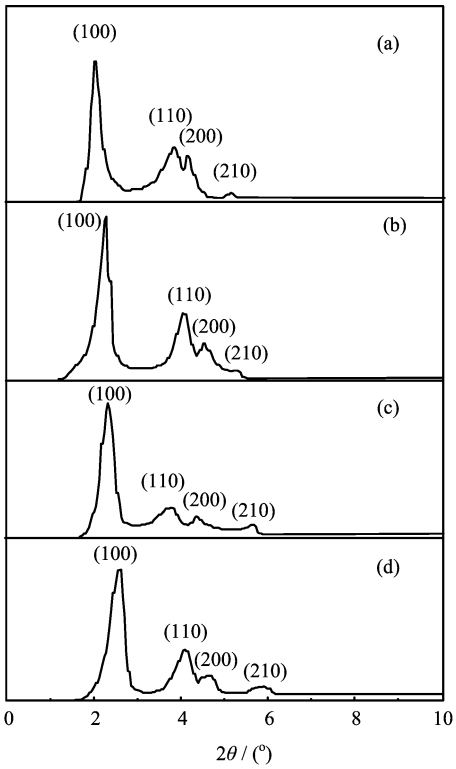

FIG. 1 XRD patterns of the samples. (a) S_2 (micrometer MCM-41, uncalcined), (b) S_2 (micrometer MCM-41, calcined), (c) S_1 (nanometer MCM-41, uncalcined), (d) S_1 (nanometer MCM-41, calcined).

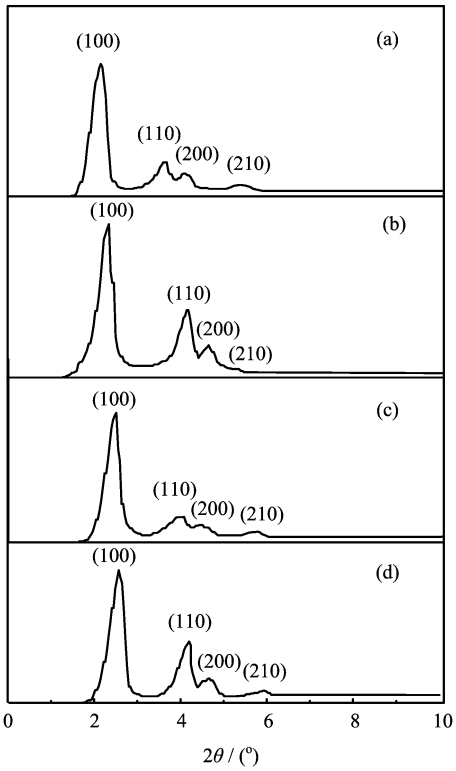

FIG. 2 XRD patterns of the samples. (a) S_2-CdS ((micrometer MCM-41)-CdS); (b) S_2 (micrometer MCM-41), (c) S_1-CdS ((nanometer MCM-41)-CdS), (d) S_1 [(nanometer MCM-41)].

ISSN 1003-7713/DOI:10.1360/cjcp2007.20(1).83.7

cess of the incorporation of the guest nanoparticles into the pores of the molecular sieves. This also indicates that the channels of the MCM-41 can serve as templates for encapsulating nanoguest materials. However, the diffraction intensity of the host in the corresponding host-guest composite material is weaker than in the MCM-41 host. This is due to the decrease in the order degree of the molecular sieve host after the CdS guest dispersed into the host. The wide-angle XRD pattern (Fig.3) for the nanometer MCM-41 containing CdS nanoparticles shows broad characteristic peaks corresponding to the CdS nanoparticles [39]. Based on the width of the diffraction peaks, the average size of the CdS nanoparticles should be less than 2.0 nm. Accordingly, CdS nanoparticles should be entrapped inside the channels of MCM-41.

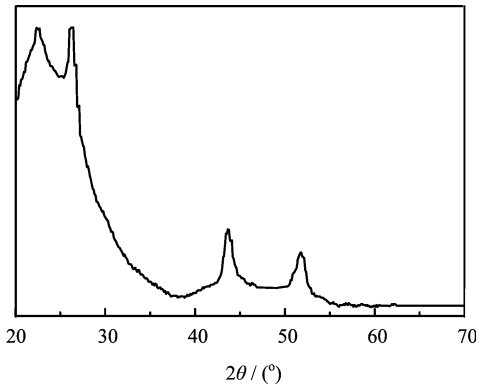

FIG. 3 Wide-angle XRD pattern of CdS nanocrystals inside the nanometer MCM-41.

C. Infrared spectra

The infrared spectra of the samples are shown in Fig.4. The Si−O−Si bond of MCM-41 can induce symmetrical and asymmetrical stretching vibrations. In addition, the Si−O−Si bond can also induce bending vibrations. The symmetrical stretching vibrations of the terminal group Si−OH are shown in the figure. The peaks at 1080, 1096, 1080, 1093 cm^{-1} are due to the asymmetrical stretching vibrations of the MCM-41. The peaks at 802, 800, 803, 799 cm^{-1} correspond to the symmetrical stretching vibrations of the Si−O−Si bond. The bending vibrations of the Si−O−Si bond are located at 449, 469, 446, 468 cm^{-1}. The bends corresponding symmetrical stretching vibrations of terminal group Si−OH are at 963, 968, 970, 967 cm^{-1}. The frameworks of composite materials are kept intact in the preparation process. However, the peaks at 1096, 968, 469 cm^{-1} for the micrometer MCM-41 (Fig.4(b)) shift toward higher wavenumber at 1080, 963, 449 cm^{-1} for the (micrometer MCM-41)-CdS sample (Fig.4(a)). The peaks at 1635, 1093, 468 cm^{-1} for the (micrometer MCM-41)-CdS sample (Fig.4(a)) shift toward higher wavenumber at 1634, 1080, 446 cm^{-1} for the (nanometer MCM-41)-CdS sample (Fig.4(c)). These changes are due to the incorporation of the guests into the MCM-41 hosts. The characteristic infrared peaks of cadmium sulfide (Fig.4(e)) [40] do not appear in the spectra of the prepared (nanometer/micrometer MCM-41)-CdS samples (Fig.4 (a) and (c)), which shows that the guests were trapped in the channels of the molecular sieves and uniformly dispersed in the MCM-41 molecular sieve hosts.

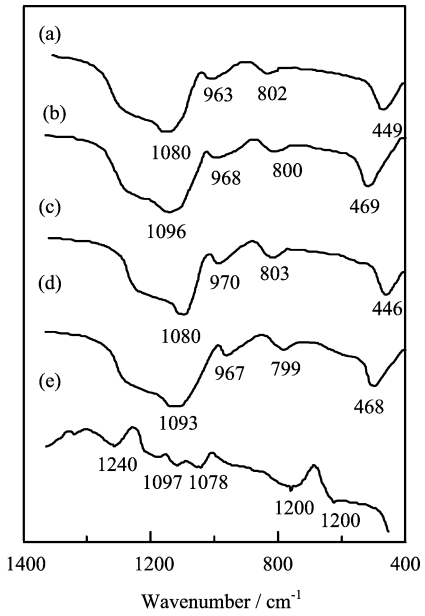

FIG. 4 Infrared spectra of the samples. (a) S_2-CdS ((micrometer MCM-41)-CdS), (b) S_2 (micrometer MCM-41), (c) S_1-CdS ((nanometer MCM-41)-CdS), (d) S_1 (nanometer MCM-41), (e) CdS.

D. Low temperature nitrogen adsorption-desorption isotherms of the samples

The low temperature nitrogen adsorption-desorption isotherms and pore size distribution patterns of the materials at the temperature of liquid nitrogen were measured, which is an effective method to characterize information about the channels of mesoporous material. The low temperature nitrogen adsorption-desorption isotherms and the pore size distribution patterns of the samples are shown in Fig.5. The isotherms can be classified as type IV isotherms according to the IUPAC (International Union of Pure and Applied Chemistry) nomenclature [41], which is a typical adsorption for mesopores materials. The surface area was measured by the Brunauer-Emett-Teller (BET) method [37] at low temperature. The obvious steep increases in the curves of Fig.5A for all four samples occur at relative pressure $0.2<P/P_0<0.4$. This increase suggests the uniformity of the mesoporous size distribution and capillary adsorption phenomena. The increases in Fig.5A(b) for the nanometer MCM-41 and

ISSN 1003-7713/DOI:10.1360/cjcp2007.20(1).83.7

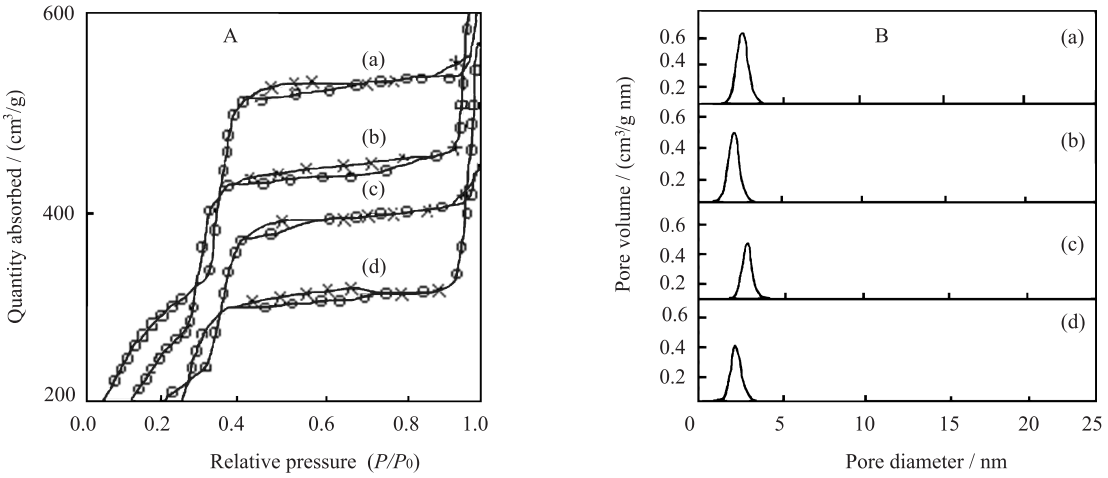

FIG. 5 Low temperature nitrogen adsorption-desorption isotherms (A) and pore size distribution patterns (B) of the samples (○ adsorption, × desorption). (a) S_2 (micrometer MCM-41, calcined), (b) S_1 (nanometer MCM-41, calcined), (c) S_2-CdS, (d) S_1-CdS.

Fig.5A(d) for the (nanometer MCM-41)-CdS samples occur at relative pressure $0.25<P/P_0<0.3$, and the increase for the micrometer MCM-41 (Fig.5A(a)) and for the (micrometer MCM-41)-CdS(Fig.5A(c)) samples are at $0.3<P/P_0<0.4$. This was caused by the difference of their pore size.

The steep increases in the curves of the composite materials are obviously less than those of the host molecular sieves. The curves of the composite materials are slightly smooth. The gradients are still big, which is caused by the good distribution of the guests in the channels of the host molecular sieves. When the relative pressure is $0.4<P/P_0<0.9$, the adsorptions in the Fig.5A do not increase obviously. The adsorption of nitrogen gas at the surface of the pore channels reaches an equilibrium, which appear as a longer adsorption terrace. The long plateau at higher relative pressures indicates that pore filling is restricted to the inflection point at $P/P_0=0.25$ for nanometer MCM-41 and (nanometer MCM-41)-CdS samples and 0.30 for micrometer MCM-41 and (micrometer MCM-41)-CdS, respectively. Other obvious steep increases, adsorbed hysteresis loops, in the Fig.5A appear at a relative pressure $0.9<P/P_0<1.0$, which is due to the capillary condensation of nitrogen gas in the big granula. The surface areas of the molecular sieves into which the guest was incorporated are still large. This is beneficial to the adsorption reaction.

The Barret-Joyner-Halenda (BJH) method [38] was applied to calculate the pore size distribution. The curves of the pore size distributions are shown in Fig.5B. The four curves of the samples are close to a Gaussian distribution, which shows that the host molecular sieves and the composite materials consist of the hexagonal array of one-dimensional uniform mesoporous channels. The pore size distributions are narrow for all four samples. The pore distributions of the nanometer MCM-41 molecular sieve and the (nanometer MCM-41)-CdS are narrower than those of micrometer MCM-41 and the (micrometer MCM-41)-CdS samples. The decreased degree of the pore sizes and surface areas of nanometer materials is a little bigger than that of the micrometer samples. This can be attributed to higher loading percentage of the guest in the (nanometer MCM-41)-CdS sample compared with the one in the (micrometer MCM-41)-CdS sample. After the guest was incorporated into the MCM-41, some parameters including surface area, pore size and pore volume decreased. The structure information about the samples derived from nitrogen adsorption data are listed in Table I. It suggests that the guests were trapped in the channels of the MCM-41 hosts.

E. Transmission electron microscopy images

The TEM image (Fig.6) shows well-ordered hexagonal arrays of mesopores and straight lattice fringes viewed perpendicular to the pore axis. It shows that the highly ordered mesoporous structure of MCM-41 remained after the formation of CdS components inside the channels of MCM-41 and no large particles located outside the mesopores were observed. The average size of the (nanometer MCM-41)-CdS sample is 90 nm.

F. UV-Vis solid state diffuse reflectance absorption spectra of the samples

The UV-Vis solid state diffuse reflectance absorption spectra of the samples are shown in Fig.7. There are no absorptions from the nanometer MCM-41 (Fig.7(a)) and micrometer MCM-41 (Fig.7(b)) molecular sieves over the range of the wavelength (200-800 nm). However, absorptions from the (nanometer MCM-41)-CdS and the (micrometer MCM-41)-CdS samples do occur. The absorption peak of bulk CdS is at 513 nm. The

ISSN 1003-7713/DOI:10.1360/cjcp2007.20(1).83.7

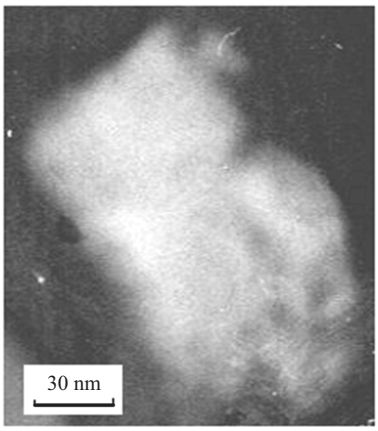

FIG. 6 TEM image of the (nanometer MCM-41)-CdS sample taken with the beam direction perpendicular to the pores.

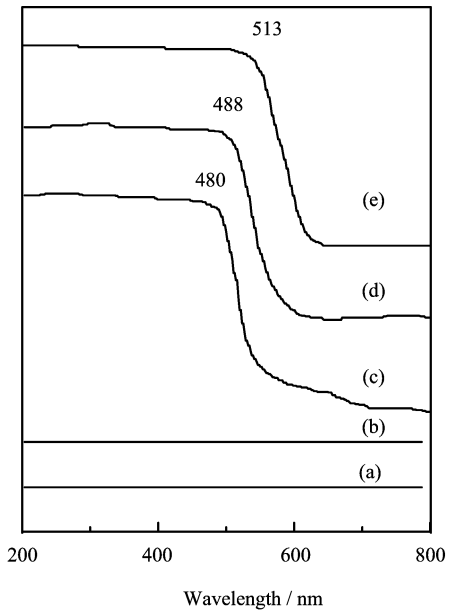

FIG. 7 Solid state diffuse reflectance absorption spectra of the samples. (a) S_1 (nanometer MCM-41, calcined), (b) S_2 (micrometer MCM-41, calcined), (c) S_1-CdS ((nanometer MCM-41)-CdS), (d) S_2-CdS ((micrometer MCM-41)-CdS), (e) CdS.

absorption peaks of the (nanometer MCM-41)-CdS and (micrometer MCM-41)-CdS samples locate at 480 and 488 nm, respectively. The absorption peaks of the (nanometer MCM-41)-CdS and (micrometer MCM-41)-CdS show the blue-shifts of 33 and 25 nm, respectively, relative to that of bulk CdS. The blue shifts result from the small size effect of the guests confined by the channels of the MCM-41 molecular sieves. The smaller the particle size of semiconductor, the more the change of the energy of the forbidden band. The particle size of semiconductor compound cadmium sulfide is smaller, but the energy of the exciting electron and hole of cadmium sulfide are higher. This results in the above blue-shifts in the solid state diffuse reflectance absorption spectra of the prepared host-guest composite materials. The energy of the forbidden bands of the CdS in the composite materials is higher than that of bulk CdS. The above phenomena further suggests that the guests were encapsulated in the channels of the MCM-41 hosts.

G. Luminescence spectra

The luminescence spectra of the samples are shown in Fig.8. The excitation peaks of the (nanometer MCM-41)-CdS and (micrometer MCM-41)-CdS are at 200 and 220 nm, respectively, and the corresponding emission peaks of the (nanometer MCM-41)-CdS and (micrometer MCM-41)-CdS samples are located at 546 and 551 nm, respectively.

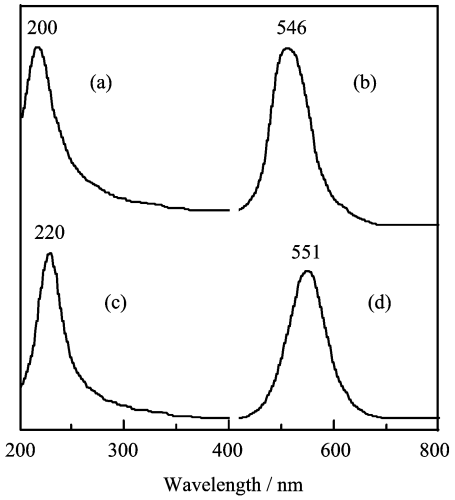

FIG. 8 Luminescence of the samples. (a) S_1-CdS ((nanometer MCM-41)-CdS), Excitation spectrum (λ_{ex}=546 nm), (b) S_1-CdS ((nanometer MCM-41)-CdS), emission spectrum (λ_{ex}=200 nm), (c) S_2-CdS ((micrometer MCM-41)-CdS), excitation spectrum (λ_{ex}=551 nm), (d) S_2-CdS ((micrometer MCM-41)-CdS), emission spectrum (λ_{em}=220 nm).

The excitation and emission spectra of the (nanometer MCM-41)-CdS and (micrometer MCM-41)-CdS have the blue-shifts of 20 and 5 nm compared with those of the (micrometer MCM-41)-CdS sample. This shows that the fluorescence excimer of the (nanometer MCM-41)-CdS is smaller than that of the (micrometer MCM-41)-CdS. Therefore, the (nanometer MCM-41)-CdS is excited with higher energy, which shows that the energy band of the (nanometer MCM-41)-CdS sample is higher than that of the (micrometer MCM-41)-CdS sample. The luminescence of the samples is weak, suggesting that the non-radiative process in the prepared samples is very strong. Therefore, the population inversion is very easily established. The luminescence bands of the (nanometer MCM-41)-CdS and the (micrometer MCM-41)-CdS samples are very broad, which results

ISSN 1003-7713/DOI:10.1360/cjcp2007.20(1).83.7

from the strong electron-photon interaction in the samples. There exists a large quantity of defects and the different types of hanging bonds in the interfaces, which results in additional defect energy levels.

V. CONCLUSION

Samples of (nanometer MCM-41)-CdS and (micrometer MCM-41)-CdS composite materials were prepared. The use of thioacetamide as a sulfur precursor avoids the toxicity of hydrogen sulfide under a hydrothermal condition. The frameworks of the prepared host-guest composite materials are retained in a highly ordered way. The combination characterization of chemical analysis X-ray diffraction, low-temperature nitrogen adsorption-desorption technique, infrared spectroscopy and solid state diffuse reflectance absorption spectroscopy showed that the guest cadmium sulfide was successfully encapsulated in the channels of the molecular sieve hosts. The prepared composite (nanometer MCM-41)-CdS and (micrometer MCM-41)-CdS samples show luminescence.

VI. ACKNOWLEDGMENT

This work was supported by the Department of Science and Technology, Ministry of Education of China (No.02044/259606).

[1] C. T. Kresge, M. E. Leonwicz and W. J. Roth, Nature **359** (6396), 710 (1992).
[2] J. S. Beck, J. C. Vartuli and W. J. Roth, J. Am. Chem. Soc. **114**, 10834 (1992).
[3] X. S. Zhao, G. Q. Lu and G. Millar, Ind. Eng. Chem. Res. **35**, 2075 (1996).
[4] E. D. Davis, Nature **417** (20), 813 (2002).
[5] A. Corma, V. Fornes and M. T. Navarro, J. Catal. **148**, 569 (1994).
[6] X. Y. Chen, L. M. Huang and G. Z. Ding, Catal. Lett. **44**, 123 (1997).
[7] A. Tuel and S. Gontier, Chem. Mater. **8**, 120 (1996).
[8] A. Corma, M. T. Navarro and J. P. Pariente, J. Chem. Soc. Chem. Commun. 147 (1994).
[9] P. T. Tanev, M. Chibwe and T. J. Pinnavaia, Nature **368**, 321 (1994).
[10] A. Poppl, M. Hartmann and L. Kevan, J. Phys. Chem. **99**, 17251 (1995).
[11] M. Hartmann, A. Poppl and L. Kevan, J. Phys. Chem. **99**, 17494 (1995).
[12] A. Sayari, I. Moudrakovski and C. Danumah, J. Phys. Chem. **99**, 16373 (1995).
[13] S. O. Brien, J. Tudor and S. Barlow, J. Chem. Soc. Chem. Commun. 641 (1997).
[14] M. N. Eswaramoorthy and C. N. R. Rao, J. Chem. Soc. Chem. Commun. 102 (1998).
[15] A. Corma, A. Martinez and V. Martinez-Soria, J. Catal. **153**, 25 (1995).
[16] X. S. Zhao and G. Q. Lu, J. Phys. Chem. B **102**, 1556 (1998).
[17] T. Maschmeyer, F. Rey and G. Sankar, Nature **378**, 159 (1995).
[18] X. Feng, G. E. Fryxell and L. Q. Wang, Science **276**, 923 (1997).
[19] D. J. Macquarrie and D. B. Jackson, J. Chem. Soc. Chem. Commun. 1781 (1997).
[20] W. D. Xia, D. Z. Wang, S. Y. Zhang, S. D. Wan, X. D. Meng and H. Wang, Chin. J. Chem. Phys. **16**, 1 (2003).
[21] Y. G. Zhang and Y. C. Chen, Chin. J. Chem. Phys. **16**, 51 (2003).
[22] H. Huang, W. Q. Zhang, C. A. Ma, X. B. Zhang, Z. H. Ge and H. M. Lu, Chin. J. Chem. Phys. **16**, 131(2003).
[23] K. Fang, S. P. Li, L. L. Cui, W. M. Mao and Q. H. Wu, Chin. J. Chem. Phys. **16**, 163 (2003).
[24] X. S. Niu, W. M. Du, W. P. Du and K. Jiang, Chin. J. Chem. Phys. **17**, 79 (2004).
[25] Y. Y. Zhang, Y. S. Yin and L. P. Ma, Chin. J. Chem. Phys. **17**, 83 (2004).
[26] A. Q. Zhou, X. H. Xu and W. F. Yao, Chin. J. Chem. Phys. **17**, 305 (2004).
[27] L. Sun, Z. J. Zhang and H. X. Dang, Chin. J. Chem. Phys. **17**, 618 (2004).
[28] Z. M. Li, F. Q. Xu and X. Y. Su, Chin. J. Chem. Phys. **18**, 117 (2005).
[29] L. P. Zhu, Z. J. Jia, Y. W. Tang, L. L. Ma and W. Y. Huang, Chin. J. Chem. Phys. **18**, 237 (2005).
[30] Q. Cai, Z. S. Luo and W. Q. Pang, Chem. Mater. **13**, 258 (2001).
[31] Z. T. Zhang, S. Dai and X. Fan, J. Phys. Chem. B **105**, 6755 (2001).
[32] X. Liu and J. K. Thomas, Langmuir **5**, 58 (1989).
[33] Y. Li, D. Xu and Q. Zhang, Chem. Mater. **11**, 3433 (1999).
[34] G. A. Ozin, A. Kuperman and A. Stein, Angew. Chem. **4**, 511 (1992).
[35] G. D. Stucky and J. E. Mac Dougall, Science **247**, 669(1990).
[36] Q. Z. Zhai and Y. C. Kim, Chin. J. Spectrosc. Lab. **15**, 82 (1998).
[37] S. Brunauer, P. H. Emmett and E. Teller, J. Am. Chem. Soc. **60**, 309 (1938).
[38] E. P. Barett, L. G. Joyner and P. P. Halenda, J. Am. Chem. Soc. **73**, 373 (1951).
[39] Y. Wang and N. Herron, Phys. Rev. B **42**, 7253 (1990).
[40] A. Richard, Q. Nyquist and O. K. Ronald, *Infrared Spectra of Inorganic Compounds*, New York & London: Academic Press, 252 (1971).
[41] IUPAC, Pure. Appl. Chem. **87**, 603 (1957).

ISSN 1003-7713/DOI:10.1360/cjcp2007.20(1).83.7